International Journal of Greenhouse Gas Control 129 (2023) 103993

Contents lists available at ScienceDirect

International Journal of Greenhouse Gas Control

journal homepage: www.elsevier.com/locate/ijggc

Multi-objective optimisation of a carbon capture and sequestration supply chain under seismic risk constraints. A case study considering industrial emissions in Italy

Daniel Crîstiu [a], Federico d'Amore [a,b], Paolo Mocellin [c], Fabrizio Bezzo [a,*]

[a] CAPE-Lab – Computer-Aided Process Engineering Laboratory, Department of Industrial Engineering, University of Padova, via Marzolo 9, Padova, PD 35131, Italy
[b] Politecnico di Milano, Department of Energy, via Lambruschini 4, Milano IT-20156, Italy
[c] Department of Industrial Engineering, University of Padova, via Marzolo 9, Padova, PD 35131, Italy

ARTICLE INFO

Keywords:
CCS
Carbon capture and sequestration
Multi-objective optimisation
Seismic risk
Industrial emissions
Supply chain

ABSTRACT

Carbon capture and sequestration represents a key decarbonisation option, particularly for large-scale fossil-based industry sectors (e.g. cement, steel, and oil refineries). Carbon capture and sequestration networks have nonetheless raised concerns regarding the possibility of leakages, especially in high seismic-risk regions.

In this study, a multi-objective mixed integer linear programming modelling framework is developed to minimise the cost and the seismic risk associated with the deployment of a carbon capture and sequestration infrastructure in Italy. The most significant industrial carbon dioxide sources (23 cement plants, 7 refineries, and 2 steel mills) are included in the model. The optimisation variables comprise capture technologies, transport options (onshore vs. offshore pipelines), and the choice of onshore and offshore deep saline aquifers for sequestration.

Three carbon dioxide emission reduction targets (20 %, 50 %, 80 %) are considered to assess the optimal design configurations in terms of either cost or seismic risk. Results show that the seismic risk optimum determines an increase in total cost ranging between 10 % (for an 80 % reduction target) and 65 % (for a 20 % reduction target) with respect to the economic optimum. Considering only offshore sequestration leads to cost increase between 20 % and 30 % with respect to solutions accepting onshore sequestration, too. Conversely, cost-optimal infrastructures have a seismic risk that is between 1.5 and 18 times higher than that of the safest chains.

1. Introduction

In the latest assessment report of The Working Group III (WG3), the Intergovernmental Panel on Climate Change (IPCC) provided an updated global assessment of mitigation progress and climate change pledges. As already stated by the WG1 in a precedent report, in the past 10 years (2010-2019), the net anthropogenic Greenhouse Gas (GHG) reached the highest levels of emissions in human history. To achieve global net zero CO_2 emissions and strengthen the global response to climate change by limiting global warming under 1.5°C (according to Paris Agreement) or to 2°C (announced by COP26), urgent and immediate mitigation actions are needed. Deep GHG emissions reduction is required in all sectors, particularly for large-scale fossil-based industry sources, such as the manufacture of cement, steel and chemicals. Carbon Capture and Sequestration (CCS) is recognised as a key decarbonisation option (IPCC, 2022): CCS comprises a series of technologies capturing CO_2 from large stationary emission sources (in this case, industries such as cement, iron and steel and refineries), and safely transporting it to geological storage into underground formations (Bui et al., 2018).

The design of optimal CCS infrastructures is a complex task, and over the last years, several studies have been published aiming at the cost-optimisation of CCS supply chains (SCs), typically adopting mixed integer linear/non-linear programming (MILP/MINLP) approaches. Just to mention some recent contributions, Nguyen et al. (2021) optimised a supply chain for carbon capture, utilisation and sequestration in Germany (CCU). Kegl et al. (2021) used a MINLP approach for the optimal design of a CCUS (carbon capture, utilisation and storage) SC, considering a hypothetical case concerning Slovenia, Croatia and Austria. Bjerketvedt et al. (2022) investigated a shipping infrastructure for enabling a CCS from the Norwegian industry, using a multi-period MILP model to minimise transport cost. Becattini et al. (2022) proposed a

* Corresponding author.
E-mail address: fabrizio.bezzo@unipd.it (F. Bezzo).

https://doi.org/10.1016/j.ijggc.2023.103993
Received 14 December 2022; Received in revised form 21 July 2023; Accepted 7 October 2023
Available online 11 October 2023

Acronyms

CCS	carbon dioxide capture and sequestration
CCUS	carbon dioxide capture, utilisation and sequestration
CDR	carbon dioxide removal
GHG	greenhouse gas
MILP	mixed integer linear programming
MINLP	mixed integer non-linear programming
SC	supply chain

Sets

k	capture technology $\{kc, kr_{1,2,3}, ks_{1,2,3}\}$
n	nodes in the model $\{c_{1-23}, r_{1-7}, s_{1-2}, z_{1-14}, v_{1-7}, e_{1-166}\}$
p	pipeline $\{p_1, p_2, p_3, p_4\}$

Scalars

α	carbon dioxide reduction target [%]
LD^{max}	threshold distance for transport arcs [km]
Ω	additional transportation cost for offshore pipeline [$\Omega = 1.75$]
K_1	parameter used to adjust the fragility with respect to the material used, pipe diameter [$K_1 = 0.6$]
Θ	additional cost for offshore sequestration [$\Theta = 2.5$]
USC	unitary sequestration cost [$USC = 7.2$ €/t]

Parameters

$CCA_{k,n}$	CO_2 avoidance costs of capture technology k used in the emitting node n [€/t]
η_k	capture efficiency of a technology k [%]
$f_{n,n'}$	cost factor for the increase in pipelines transport costs due to obstacles for transport arc n-n'
fix_k^{CCA}	fixed cost component of capture plant k [%]
$IN_{0,k}$	reference-case yearly captured flowrate through technology k [t/y]
$LD_{n,n'}$	matrix of distances between node n and n' [km]
η_k	capture efficiency for technology k [%]
PVG_n	peak ground velocity [m/s^2]
Q_p	transported capacity discretisation according to set p [t of CO_2]
$RR_{n,n'}$	repair rates
ρ_k	rate of additional CO_2 emissions of a technology k due to energy requirements [-]
S_{A_n}	spectral acceleration [g]
τ_n	cost factor for obstacles description in node n
UTC_p	unitary transport cost for size p [€/km/t]
var_k^{CCA}	variable cost component of capture plant k [%]
X_n	longitude of node n [rad]
Y_n	latitude of node n [rad]

Continuous variables

$IN_{k,n}$	annual captured CO_2 flowrate through technology k in the emitting node n [t/y]
OUT_n	annual sequestered quantity of CO_2 [t/y]
$Q_{q,n,n'}$	carbon flowrate of size p transported from n *to* n' [t of CO_2]
TC	total cost [€/y]
TCC	total capture cost [€/y]
TR	total seismic risk [ruptures/y]
TSC	total sequestration cost [€/y]
TTC	total transport cost [€/y]

Binary variables

$\lambda_{p,n,n'}$	1 if flowrate p is transported between nodes n and n', 0 otherwise

MILP model that minimises the total cost of a national-wide CCS SC of Switzerland's waste-to-energy sector, introducing into the optimisation algorithm the dynamic development over a time horizon of 25 years. On a continent-wide scale, d'Amore et al. (2021a) used a MILP framework for the economic optimisation of a large-scale CCS SC, considering the European energy and industrial (cement, steel, refining) sectors as emissions sources, later also focussing on the impact of ship transport (d'Amore et al., 2021b). Ostovari et al. (2022), defined a MILP model at a European level for designing a climate-optimal CCUS SC, considering mineralisation as the storage option. On a global scale, using a source-sink matching model based on a linear programming formulation for the objective function, Wei et al. (2021) proposed a cost-effective CCUS layout in line with the target of limiting the temperature to 2°C.

The deployment of large-scale CCS networks and long-distance underground pipelines for CO_2 transportation has nonetheless raised concerns regarding the possibility of leakages, potentially increasing the technology cost (Chen et al., 2022). The problem of risk in CCS SC design and optimisation has been considered in a limited number of studies. For instance, Lee et al. (2017) combined environmental and financial risk in the economic optimisation of the CCS SC network. d'Amore et al. (2018) integrated societal risk due to hazards into the MILP model of a CCS SC, specifically evaluating the impact of the risk mitigation actions on the total transport cost. d'Amore et al. (2020) introduced the idea of social acceptance into the design of a European CCS SC, acknowledging that the effective deployment of CCS technologies and their actual cost may depend on the risk perception of local communities. Al-Yaeeshi and Al-Ansari (2022) incorporated risk management for a resilient design of a proposed CO_2 to deal with disruptions that can lead to production and economic losses.

When considering the Italian Peninsula, specific risk is related to its high seismicity profile. This can have negative impacts on the installation of underground CO_2 pipelines. Infrastructures and pipeline networks deteriorate because of many factors, including external environmental conditions, and they are vulnerable to various natural hazards, such as earthquakes. Earthquake-induced damage to pipeline networks, especially buried, may lead to severe failures, important economic losses to asset owners, and environmental impact on society (Tsinidis et al., 2020). The resilience of such extended systems under extreme natural events, including earthquakes, must be carefully considered, mainly when hazardous materials are transported, as in the case of natural gas pipelines or carbon dioxide pipelines (Lanzano et al., 2014).

Therefore, this study aims at bridging this gap in the design of CCS infrastructures by integrating the seismic risk associated with the transportation stage as part of the optimisation framework. This will bring valuable insights and can also help deal with the unstable risk perception toward CCS projects that the general public may have. This study proposes a Multi-Objective MILP modelling framework of a national-wide supply chain for a CCS technology that simultaneously minimises the Total Cost and the Total Seismic Risk associated with the underground pipeline network used for CO_2 transportation. The study focuses on the decarbonisation of the Italian industry, considering the CO_2 emissions coming from large stationary CO_2 emissions, i.e. 23 cement plants, 2 steel mills, and 7 refineries. The overall annual CO_2 emissions considered in the model add up to about 34 Mt/y, representing 90 % of the total Italian emissions from these sectors. Multiple scenarios are defined based on different carbon reduction target aiming to capture and sequester 20 %, 50 % and 80 %, respectively, of the industrial emissions.

The article is organised as follows. First, materials and methods are explained, and seismic risk is defined. The next section will elaborate further on the mathematical formulation, introducing the modelling

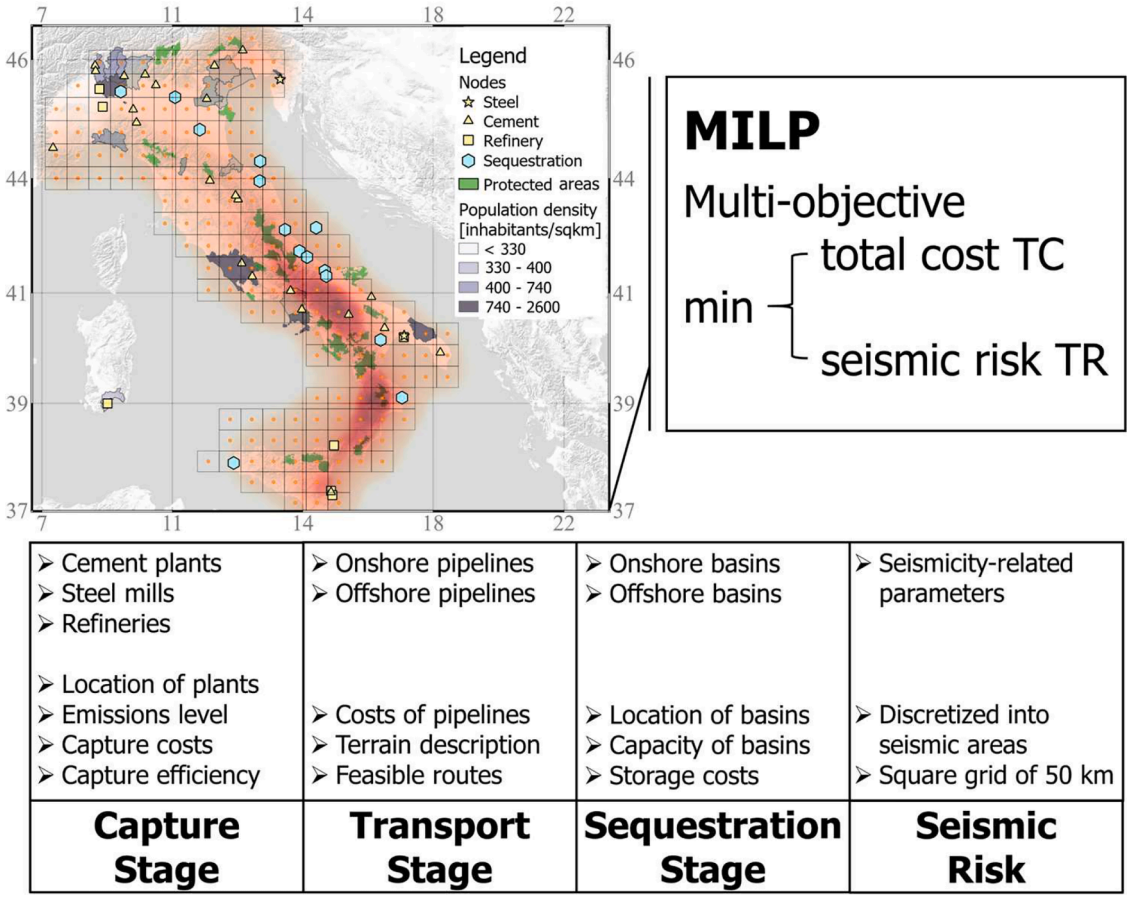

Fig. 1. Graphic representation of the multi-objective CCS SC model considered in this study.

assumptions and inputs, and the modelling framework. Then, the optimisation results will be presented and discussed. Some final remarks will conclude the article.

2. Material and methods

The proposed multi-objective MILP model for economic and seismic risk optimisation of a nation-wide CCS SC incorporates decisions about capture technologies, pipelining (both onshore and offshore pipelines) and sequestration (both onshore and offshore saline aquifers). CO_2 sources (cement plants, steel mills and refineries) and sinks are characterised by geographical coordinates and expressed as nodes in the MILP model. The seismicity parameter is discretised into a 50 km square grid that represents the Italian peninsula, each square being defined around the centre point that is considered a node in the model and is characterised by geographical coordinates. Economies of scale are implemented for both capturing technologies and pipelines, for the latter using discrete pipeline diameters with the corresponding capacities and costs. A graphic representation of the methodology and the multi-objective, multi-echelon MILP model is presented in Fig. 1.

2.1. Definition of seismic risk

The high seismic activity of the Italian peninsula may influence the deployment of CCS technologies. This study aims at providing a rational and evidence-based decision of installing the pipelines within the transport stage of an Italian CCS SC from large stationary industrial emission sources, also including the impact of seismic risk performance.

Historically, pipelines have suffered heavy damage due to seismic load, as in the case of the Northridge earthquake of 1994 (USA), Kobe in 1995 (Japan), and Chi-Chi earthquake in 1999 (Taiwan) (Germoso et al., 2021). Even more recently, pipeline systems worldwide have suffered severe failures due to seismic actions, e.g. during the devastating Tohoku earthquake of 2011 (Japan), in New Zealand (2010) and Chile (2010). In this framework, the Italian peninsula is a seismic-prone area, as well, and severe failures to pipelines have been reported because of seismic scenarios, as in the case of the L'Aquila earthquake (2009) and the earthquake of Emilia (2012) (Lanzano et al., 2015).

The structural performance of pipelines mainly depends on the interaction between the soil and the pipe segment itself. Critical factors include the shear strength properties of the soil and the variability in ground motion parameters (e.g. wave propagation length, ground particle velocity, wave velocity, etc.) (Wijaya et al., 2019). Many empirical relations were developed to describe the structural performance during a seismic action, and the most significant relies on a concise set of parameters which include the Peak Ground Acceleration and the Peak Ground Velocity (Eidinger, 1998; O'Rourke and Deyoe, 2004). Such parameters are used in seismic risk assessment to evaluate the likelihood of exceeding a specific threshold from the total range of earthquake hazards, producing a vulnerability (Honegger and Wijewickreme, 2013). From the severity perspective of an earthquake ground shaking, probabilistic methods consider the variability in the size, recurrence interval, and location of earthquakes in a region. Lanzano et al. (2015) summarised the damage patterns occurring in pipelines that depend on the properties of materials and joint features.

The seismic damage on pipelines induced by an earthquake is typically given in terms of performance indicator curves, which are functions of the seismic intensity. The Repair Rate is commonly adopted among the developed performance indicators. It gives the number of repairs after an earthquake of a given intensity for a unit length of the pipeline (Tromans, 2004). Associated curves are mainly obtained from the best fitting of collected data in a post-earthquake scenario. Also, the

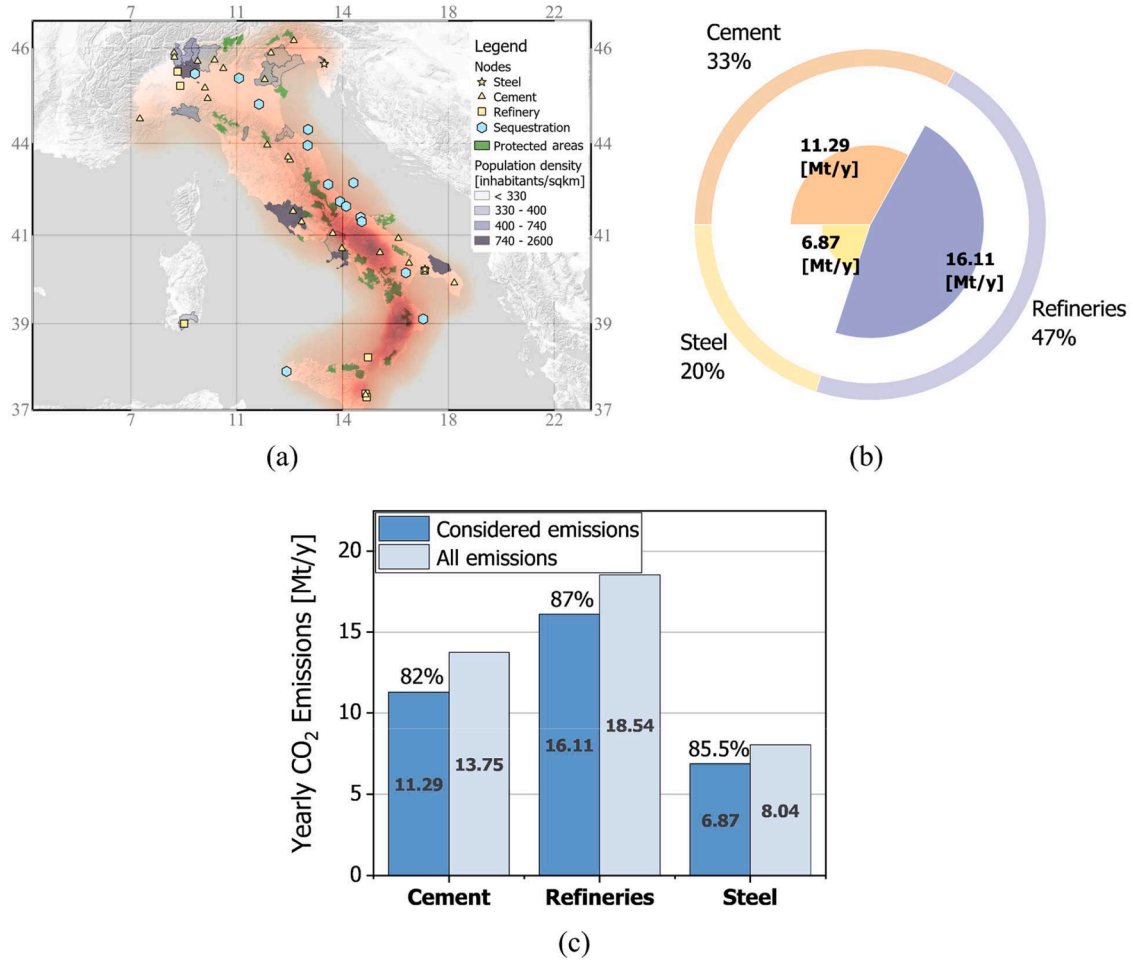

Fig. 2. (a) Geographical location of the CO_2 emission sources and geological sequestration sites; (b) Subdivision on emitting sectors of the total CO_2 emissions considered in the model; (c) Comparison with total sectorial Italian emission in 2019 (EEA, 2020).

concept of fragility function is broadly used. It provides the probability of exceedance of a given damage state as a function of a parameter linked to the seismic action (Mina et al., 2020). Such approaches provide a prediction of the damage or the failure probability by considering the uncertainty of earthquake features (ALA, 2001; Eidinger, 1998; O'Rourke and Ayala, 1993). Ultimately, fragility curves represent a relationship between the measure of the seismic action and the probability of achieving a class of damage (e.g. slight, moderate, severe damage) (Argyroudis and Pitilakis, 2012).

These components, i.e. the likelihood and the impact of a seismic action, are ultimately used for the Quantitative Risk Analysis, which allows evaluating risks towards an optimal pipeline performance and reliability design.

3. Mathematical formulation

3.1. Modelling assumptions and inputs

The multi-objective MILP modelling framework is formulated to simultaneously optimise the economic (i.e., minimum cost) performance of a CCS SC and the seismic (i.e., minimum risk) performance of the pipeline system. The CO_2 sources included in the model are defined as follows: in the case of the refining and steel sectors, all locations with yearly emissions larger than or equal to 1 Mt CO_2/y are included in the model, while for cement plants, which are smaller and more distributed, the threshold is lowered to 0.3 Mt CO_2/y (Fig. 2). These thresholds of minimum of emissions are set so as to comprise at least 80 % of the yearly CO_2 emissions in each industrial sector (Fig. 2c). Yearly CO_2 emission levels for each industrial node refer to the year 2019 and, together with the exact geographical coordinates of the emitting nodes, were retrieved from EEA (2020). Upon being captured from emission points, CO_2 is transported to geological basins, which can be either onshore or offshore and are represented in Fig. 2a as sequestration nodes.

The spatially-explicit features are described as nodes in the model through the set n comprising:

- $n = \{c_{1-23}\} \equiv$ *cement* describing 23 cement plants nodes that are emitting altogether 82 % of the total yearly Italian CO_2 emissions from the cement sector
- $n = \{r_{1-7}\} \equiv$ *refinery*, describing 7 refineries nodes that are emitting altogether 87 % of the total yearly Italian CO_2 emissions from the refinery sector
- $n = \{s_{1-2}\} \equiv$ *steel*, describing 2 iron and steel nodes that are emitting altogether 86 % of the total yearly Italian CO_2 emissions from steel mills
- $n = \{z_{1-14}\} \equiv$ *seque*, describing 14 sequestration nodes, of which 3 are offshore; all sequestration nodes are deep saline aquifers (Donda et al., 2011)
- $n = \{e_{1-166}\} \equiv$ *seismic*, describing 166 seismic nodes obtained by the discretisation of the dataset of seismic parameters (Stucchi et al., 2011)

The exact geographic coordinates for each CO_2 emitting source

Table 1
Obstacles related to the terrain description and the multiplicative cost factor increasing the pipeline installation costs.

Description of obstacle	Cost factor τ_n [-]
No obstacle	1
Protected areas (Herzog and Javedan, 2009)	
Populated places	15
National Parks	30
Regional Parks	15
Elevation (Kim et al., 2018)	
Elevation 1 (0-100 m)	1
Elevation 2 (100-300 m)	1.1
Elevation 3 (300-500 m)	1.3
Elevation 4 (500-700 m)	1.5
Elevation 5 (700-900 m)	1.7
Elevation 6 (900-1100 m)	1.9
Elevation 7 (1100-1300 m)	2
Elevation 8 (1300-1500 m)	3
Elevation 9 (1500-1700 m)	4
Elevation 10 (>1700 m)	5

Table 2
Scenario description: Scenario I include 3 sub scenarios, I.1, I.2, I.3, that differ in the CO_2 target α, allowing onshore and offshore sequestration in the Italian saline aquifers. Scenario II analyses the case of offshore sequestration in the Italian saline aquifers with α = 80 %. Total captured CO_2 represents the CO_2 flowrate that is captured from all sectors to reach the target α, while Total sequestered CO_2 contains also the additional CO_2 emissions due to capture plants.

Scenario	Case	α	Total Captured CO_2	Sequestration		Total Sequestered CO_2
		[%]	[Mt/y]	Onshore	Offshore	[Mt/y]
I.1	a	20	6.87	v	v	8.24
	b		6.89			7.81
	c		6.86			6.88
I.2	a	50	17.14	v	v	19.74
	b		17.24			19.22
	c		17.16			18.56
I.3	a	80	27.47	v	v	31.06
	b		27.57			31.17
	c		27.45			30.91
II	a	80	27.57		v	31.17
	c		27.45			30.91

(subsets *cement, refinery, steel*), with their corresponding level of emissions (IN_n^{max}), as well as the locations and capacities of geological storage basins (subset *seque*), and the exact coordinates of each seismic node (subset *seismic*) with the corresponding averaged value for the seismic parameter, are reported in the Supplementary Material. Each node in set n is described by its exact coordinates X_n [longitude] and Y_n [latitude].

3.1.1. Capture plants

A comprehensive description of the capture options, represented by different capture technologies tailored to each industry and a detailed explanation of the methodology used, can be found in d'Amore et al. (2021a). The capture problem is modelled by a set $k = \{kc, kr_{1,2,3}, ks_{1,2,3}\}$ containing:

- $k = \{kc\} \equiv$ capture technology referred to CO_2 capture from cement plants. In this case, a single CO_2 capture technology is assumed, i.e. oxy-fuel combustion with its corresponding techno-economic parameters, as this technology proved to be less expensive than amine-based separation (Gardarsdottir et al., 2019; Voldsund et al., 2019);
- $k = \{kr_{1,2,3}\} \equiv$ the three capture steps referred to CO_2 capture from refineries through monoethanolamine (MEA) based post-combustion capture, given its relatively competitive costs, potentially high efficiency, and high retrofittability. As refineries have multiple CO_2 emission points, based on d'Amore et al. (2021a) the following subdivision is proposed, in which the same capture technology (MEA-based post-combustion capture) is designed for progressively increasing steps of captured CO_2: $step_1 \equiv kr_1$: CO_2 generated by methane reformer (SMR) (IEAGHG, 2017); $step_2 \equiv kr_2$: $step_1$ and the additional CO_2 emissions from energy generation on power plant (SMR+PP) (NETL, 2015); $step_3 \equiv kr_3$: implies the use of $step_2$ and the capture of additional CO_2 emissions from other sources in the refinery (SMR+PP+Others) (van Straelen et al., 2010);
- $k = \{ks_{1,2,3}\} \equiv$ the three capture steps referred to CO_2 capture from steel mills, assumed through MEA-based post-combustion capture as

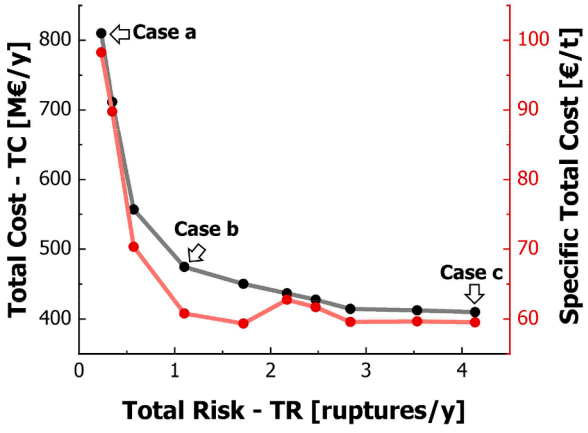

Fig. 3. Pareto front: Scenario I.1 (α = 20 % carbon reduction target): obtained through epsilon constraint method. Case a, Case b, Case c representing the three trade-off solutions (between the two objective functions: total cost TC [M€/y] and total seismic risk TR [ruptures/y]), to be discussed in detail.

Table 3
Scenarios I, II: results: Specific total cost (TC [€/t]), specific capture cost (TCC [€/t]), specific transport cost (TTC [€/t]), specific sequestration cost (TSC [€/t]), total seismic risk (TR [ruptures/y]), total pipeline system length (Tot. Length [km]). Specific costs refer to tonnes [t] of sequestered CO_2.

Scenario	Case	α	Economic results				Risk results	
			TC	*TCC*	*TTC*	*TSC*	*TR*	*Tot. Length*
		[%]	[€/t]	[€/t]	[€/t]	[€/t]	[rup./y]	[km]
I.1	a	20	98.3	82.4	8.7	7.2	0.23	390
	b		60.8	52.2	1.4	7.2	1.10	213
	c		59.5	48.3	4.0	7.2	4.14	786
I.2	a	50	85.2	70.8	7.2	7.2	1.76	788
	b		73.0	59.5	6.3	7.2	5.61	1402
	c		67.4	52.0	8.2	7.2	16.35	2921
I.3	a	80	93.5	72.2	14.1	7.2	11.17	2347
	b		87.4	72.1	8.1	7.2	12.23	2594
	c		84.5	70.5	6.8	7.2	16.48	2979
II	a	80	122.0	72.1	31.9	18.0	17.03	3296
	c		103.0	70.5	14.5	18.0	25.50	4003

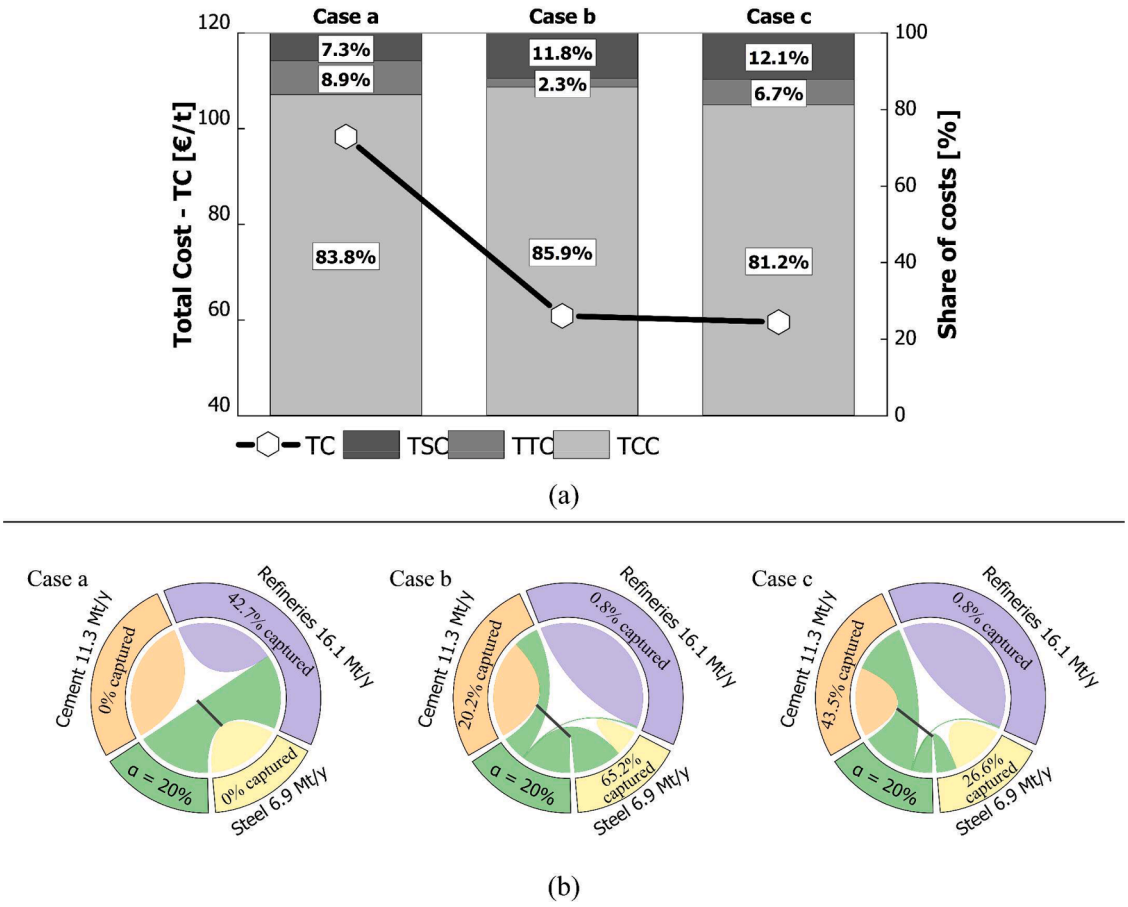

Fig. 4. Results for Scenario I.1: (a) Bars represent the cost breakdown: capture cost *TCC* [%], transport cost *TTC* [%], sequestration cost *TSC* [%] (right y-axis); the total cost *TC* [€/t] is represented by the thick solid line (left y-axis); (b) The plots show the percentage of CO_2 captured from each sector, and the contribution of each sector to total CO_2 avoided through all technologies to reach the pre-set target of $\alpha = 20$ % for the three Pareto optimal solutions (*Case a, Case b, Case c*); for example, the plot concerning *Case c* shows that the contributions to the avoided CO_2 target (green fluxes to the $\alpha = 20$ % arc) mainly derive from the steel industry and the cement one, and only in minor part from refineries. The CO_2 emissions per industrial sector are represented by the three arcs (the yearly CO_2 emissions per sector are shown [Mt/y]). The percentages of captured CO_2 from each sector account only for the directly captured CO_2 coming from the respective sector, and not also for the additional CO_2 emissions due to the capture plant.

in the case of refineries. In a steel mill, there are multiple CO_2 emission points, namely from the blast furnace, coke ovens, power plant, sinter plant, lime kiln, stoves, coke ovens and sinter plant: $step_1 \equiv ks_1$: absorption capture from power plant stack; $step_2 \equiv ks_2$: implies the use of $step_1$ and additional CO_2 emissions from blast furnace stoves and coke oven flue gas are captured through absorption; $step_3 \equiv ks_3$: implies the use of $step_2$ and additional CO_2 emissions from sinter plant are captured through absorption (Ho et al., 2013).

The rationale behind the selection of specific CO_2 capture technology for each industry (cement, refinery and steel) and the techno-economical parameters in the capture problem have been discussed in the work by d'Amore et al. (2021a). The key parameters are here summarised:

- the CO_2 avoidance costs $CCA_{k,n}$ [€/t] of capture technology k used in the emitting node n (including both a fixed component fix_k^{CCA} [%] and a variable component var_k^{CCA} [%]);
- the capture efficiency of a technology k: η_k [%];
- the rate of additional CO_2 emissions of a capture plant k due to capture energy requirements (e.g., the energy required to generate low pressure steam to fulfil the MEA heat requirement): ρ_k [-]: $\rho_k = 1$ if no additional emissions are generated by a technology k, $\rho_k = 1.2$ otherwise;
- the reference-case yearly captured flowrate $IN_{0,k}$ [t/y] (i.e., CO_2 emissions without capture) needed to scale costs over a technology k.

The infrastructure costs, as described in d'Amore and Bezzo (2017), consider OPEX and annualised CAPEX costs accordingly. Techno-economical parameters for the capture problem are summarised in the Supplementary Material.

3.1.2. Transport options

In this study, it is assumed that the captured CO_2 is transported from sources (emitting nodes) to sinks (sequestration sites) by means of pipelines, either onshore or offshore. The matrix of distances between two nodes $LD_{n,n'}$ is calculated using the spherical law of cosines, assuming a spherical Earth (d'Amore and Bezzo, 2017). Since in the discretisation approach for seismic risk, the square grid is of size of 50 km, the transportation arcs are constrained to be less than or equal to 55 km, using the seismic nodes in the transport grid.

Pipeline transport is discretised into the model through a set $p = \{p_1, p_2, p_3, p_4\}$, containing 4 different ranges of CO_2 flowrates that can be transported. For each component of the set p, a range $[Q_p^{min}, Q_p^{max}]$ [t/y] is defined. The Unitary Transportation Cost UTC_p [€/km/t] corresponding to the admissible flowrate ranges are calculated by Rubin et al. (2015) and updated through CEPCI 2018 and are presented in the Supplementary Material. The unitary transportation cost for offshore pipeline transportation is derived from onshore UTC_p through a

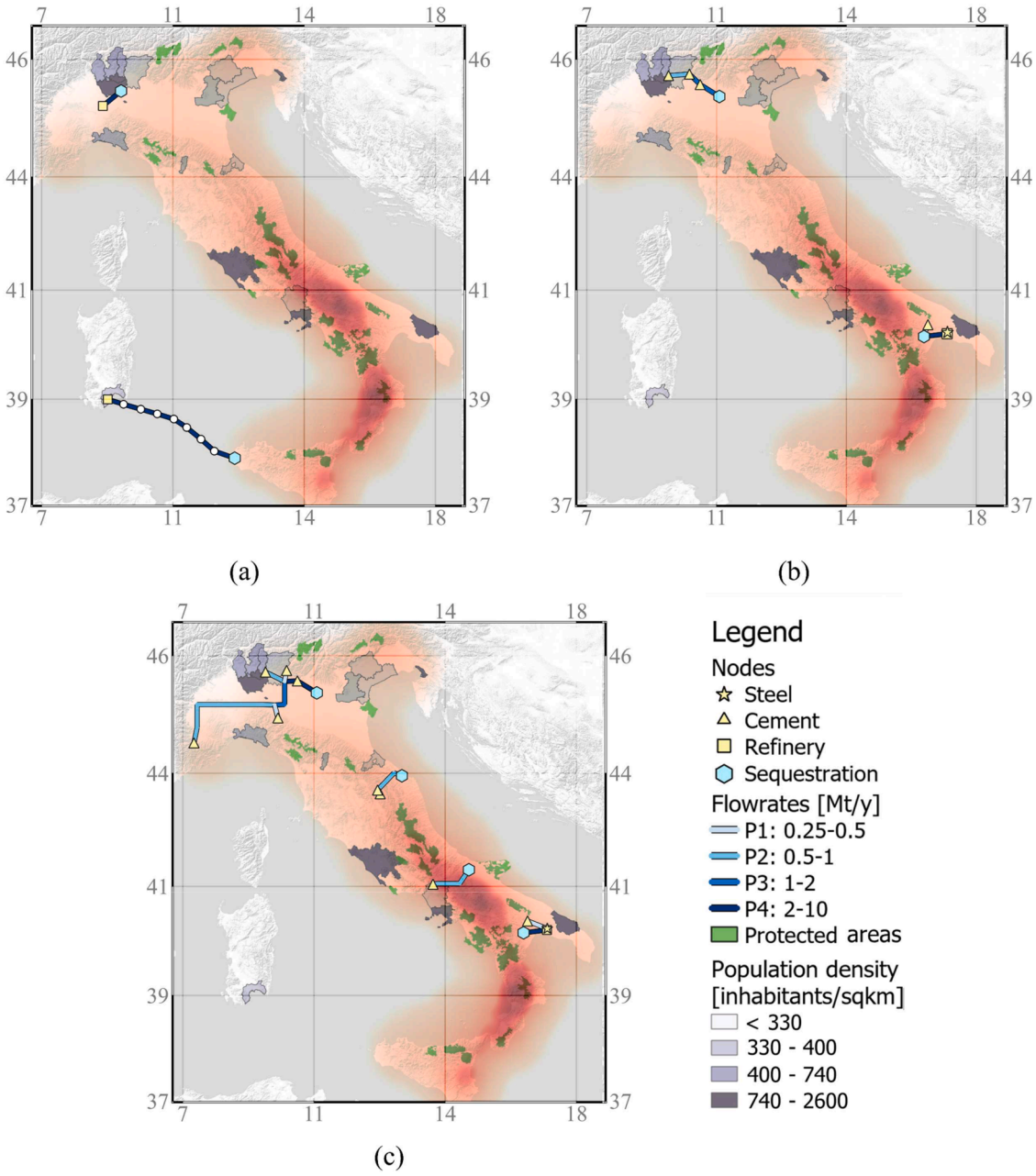

Fig. 5. Scenario I.1: CCS SCs configuration for (a) Case a: safest infrastructure, (b) Case b: trade-off configuration, (c) Case c: cheapest infrastructure.

multiplicative factor Ω [= 1.75] (d'Amore et al., 2021a). Transportation arcs are considered to be offshore if they fall in the discretised offshore areas defined by a subset $offshore_n$.

In addition, pipeline construction costs vary significantly depending on the terrains the pipelines need to be installed into, e.g. protected areas (national or state parks), populated places, and mountain landscape. To deal with this problem, a cost factor τ_n is considered in the transport problem to account for the increase in construction costs when pipelines are installed in a "difficult" landscape (Table 1). A multiplicative factor $f_{n,n'}$ is used to account for cost factors in a transport arc *n*-*n'*:

$$f_{n,n'} = \frac{1}{2}\left(\sum_i \tau_{i,n} + \sum_i \tau_{i,n'}\right) \quad i = type\ of\ obstacle\ in\ node\ n,\ \forall n, n' \tag{1}$$

The cost factors for the protected areas (national parks and populated areas) are retrieved from the study of Herzog and Javedan (2009), while for different altitudes, according to their degree of elevation, the work of Kim et al. (2018) is used. The population density in each local administrative unit is calculated based on the number of inhabitants residing per square kilometre (ISTAT, 2022a, 2022b). Only national and regional parks with an area over 25000 [ha] are selected; data are retrieved from Italian Government (2010). For each node, the elevation is referred to the coordinates of that same node.

3.1.3. Sequestration sites

The choice of the sequestration sites is based on the study by Donda et al. (2011) that assessed the geographical location and storage capacity of 14 deep saline aquifers at the Italian level, offering a detailed description of the selected sequestration sites and also assessing the seismic profile of the area occupied by the selected deep saline aquifers. The study was based on the EU GeoCapacity Project (2009). In Donda et al. (2011), the effective storage capacity of the 14 deep saline aquifers ranges between 2950 [Mt] and 11800 [Mt], calculated on the basis of the storage efficiency that ranges from 1 % to 4 %, respectively. In this

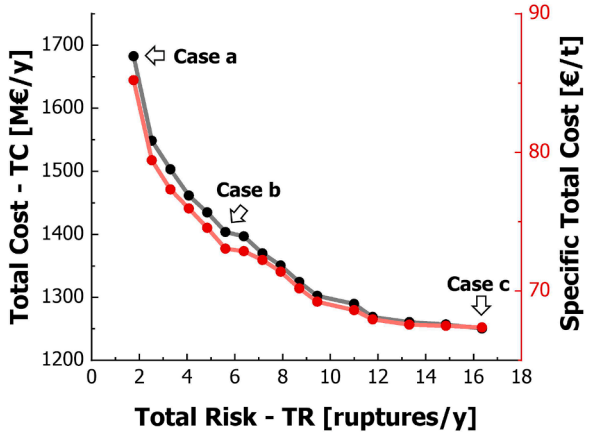

Fig. 6. Pareto front: Scenario I.2 (α = 50 % carbon reduction target): obtained through epsilon constraint method. Case a, Case b, Case c representing the three trade-off solutions (between the two objective functions: total cost TC [M€/y] and total seismic risk TR [ruptures/y]), to be discussed in detail.

study, the overall effective storage capacity is 5896 [Mt], of which 3034 [Mt] is the capacity of the offshore basins, calculated with a storage efficiency of 2 % (a value suggested in the EU GeoCapacity Project (2009)). Taking into account the overall emissions of the model (i.e. 34.3 [Mt/y]), the 14 saline aquifers would be available for 172 years, while for the scenario in which only offshore sequestration is allowed, the three offshore saline aquifers can provide the storage of overall CO_2 emissions of 89 years. A summary of the effective storage capacity of each saline aquifer is presented in the Supplementary. A key economical parameter is the unitary sequestration cost *USC* [= 7.2 €/t] retrieved from Rubin et al. (2015) and updated to year 2018 through CEPCI (2018); parameter Θ [= 2.5] accounts for the increased cost in installation and operation of offshore sequestration (ZEP, 2011).

3.1.4. Seismic risk characterisation

This study is based on a previous assessment of the fragility of gas and oil networks made by Gehl et al. (2014), which can also be used for the CCS pipeline network due to similarity in pipeline transport. In the mentioned study, the vulnerability to the buried pipelines is quantified in terms of repair rates, i.e. number of repairs per km, according to the formulation proposed by ALA (2001). Repair rates are computed as a function of the peak ground velocity and of a parameter K_1 that accounts for the fragility of the material being used and for pipe diameter. A value of K_1 = 0.6 is chosen here, assuming carbon steel as the construction material (IPCC, 2005), and by classifying the pipeline diameter as "small" (4–12 [inch]) (ALA, 2001).

The seismicity-related parameters over the entire Italian peninsula, i.e. the spectral accelerations, are obtained through a dataset containing the coordinates of polling points computed by the Istituto Nazionale di Geofisica e Vulcanologia–INGV (Stucchi et al., 2011). The maximum expected spectral acceleration in 50 years with a 10 % exceedance probability is evaluated in 16852 points. The Italian peninsula is discretised into 166 seismic nodes, which represent the centre points (seismic nodes) of the 50 km squares in the grid; the spectral acceleration S_{A_n} [g] of a seismic node is averaged over all polling points

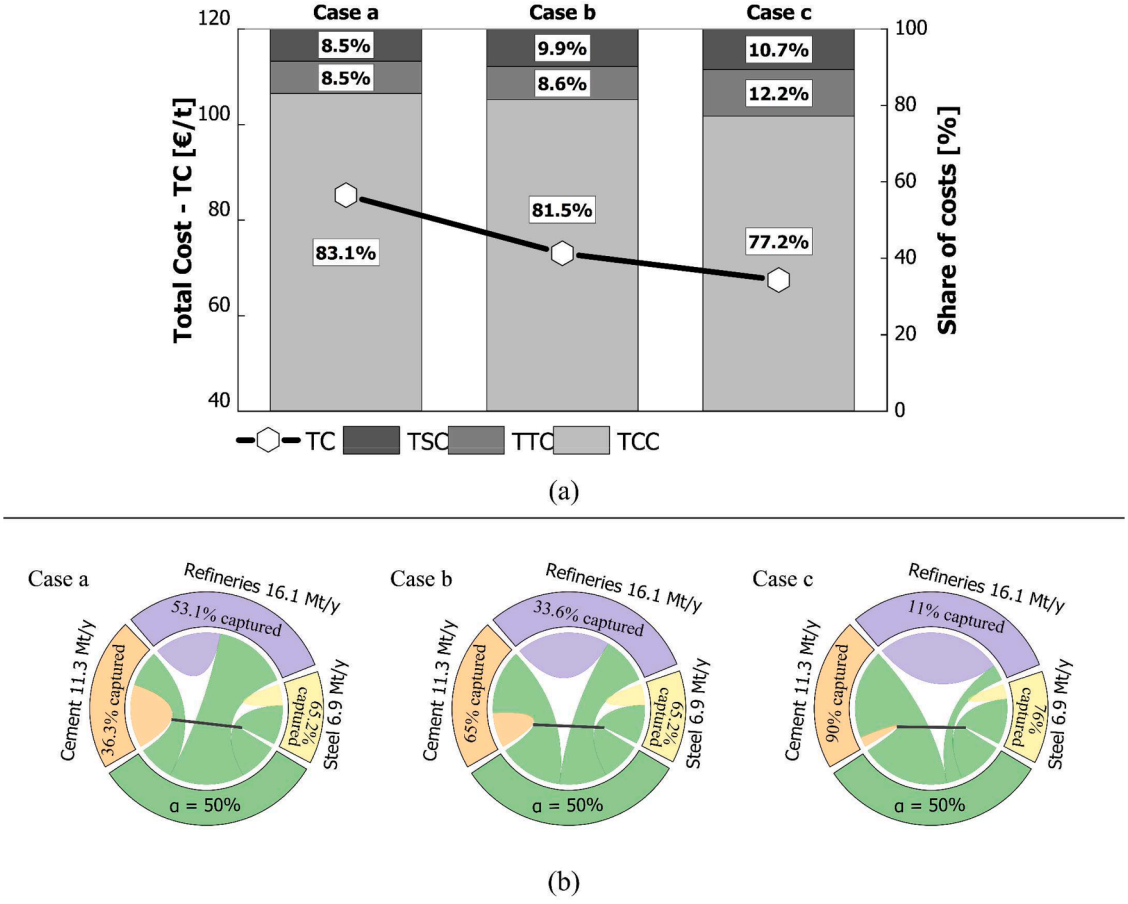

Fig. 7. Results for Scenario I.2: (a) Cost breakdown: TCC [%] capture cost, TTC [%] transport cost, TSC [%] sequestration cost (right y-axis), over total cost TC [€/t] (thick solid line, left y-axis); (b) Percentage of CO_2 captured from each sector, and the contribution of each sector to total CO_2 avoided through all technologies to reach the pre-set target of α = 50 % for the three Pareto optimal solutions (Case a, Case b, Case c).

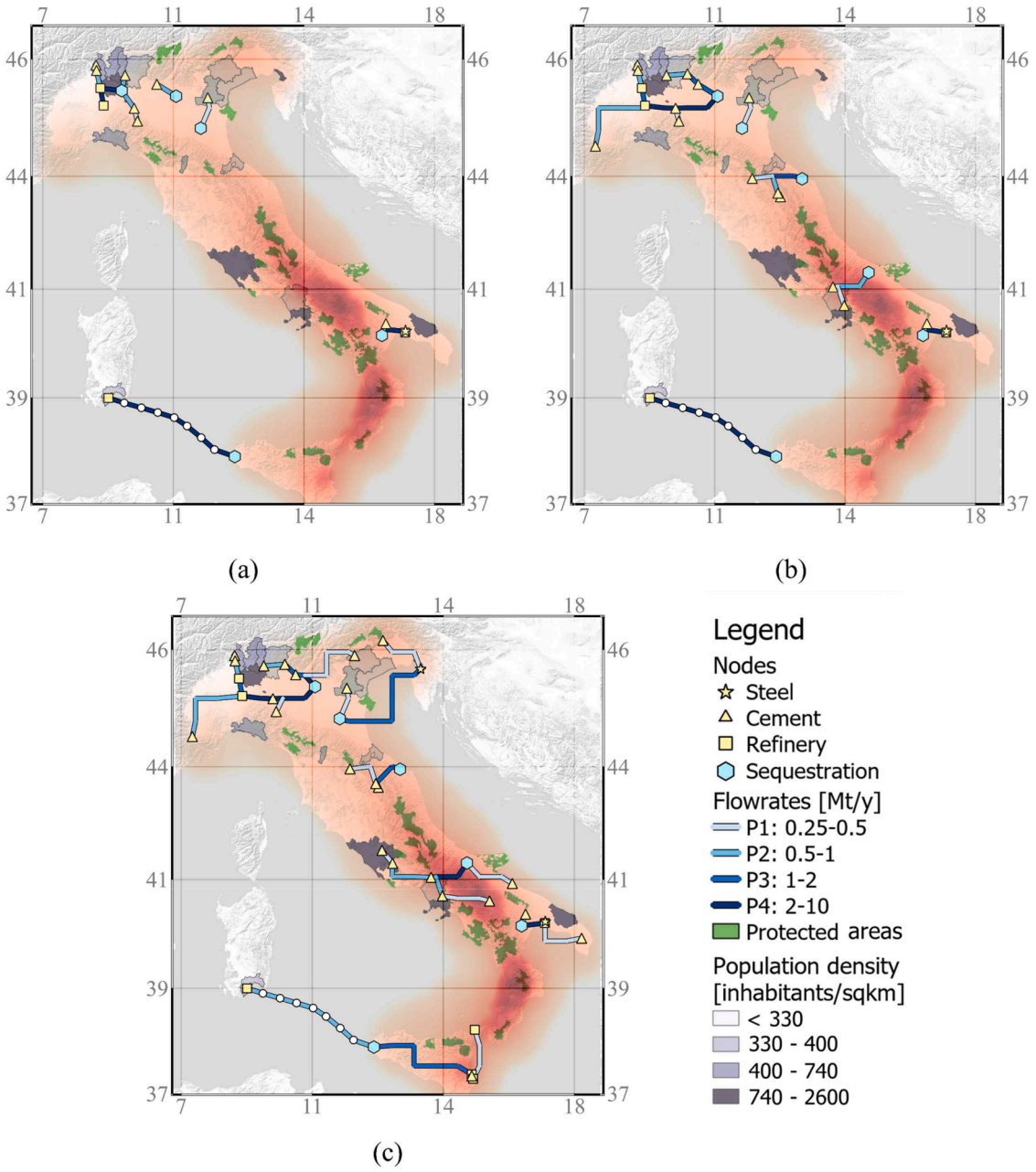

Fig. 8. Scenario I.2: CCS SCs configuration for (a) Case a: safest infrastructure, (b) Case b: trade-off configuration, (c) Case c: cheapest infrastructure.

comprised in the 50 km square around the centre point.

The repair rate $RR_{n,n'}$ is defined for every couple of nodes n and n', and calculated as follows:

$$RR_{n,n'} = 0.002416 \cdot K_1 \cdot LD_{n,n'} \cdot \max\{PGV_n; PGV_{n'}\} \ \forall n, n' \quad (2)$$

where PGV_n is the peak ground velocity computed from the spectral acceleration data according to the formulation proposed by Allen et al. (2007):

$$PGV_n = (386.4 \cdot S_{A_n})/(2\pi \cdot 1.65) \quad (3)$$

Eqs. (2) and (3) are empirical functions retrieved from the cited literature, where a more comprehensive description of the equations and their meaning is given. 0.002416 is a scaling factor (ALA, 2001); 386.4: is derived from the conversion factor between acceleration in gravity units (g) and velocity in centimetres per second (m/s) (Allen et al., 2007). These empirical functions are all based on empirical data collected from post-earthquake observations. The other nodes in set n (i.e. the nodes that do not belong to subset *{e1–166}* of seismic nodes) are assigned a value of S_{A_n} (and of PGV_n) equal to that of the seismic node at the centre of the grid square they lie within.

3.2. Modelling framework

The proposed MILP modelling framework is a multi-objective mathematical program that aims at simultaneously minimising the Total Cost *TC* [€/y] of the CCS scheme and the Total Seismic Risk *TR* [ruptures/y] of the pipeline network installation:

$$objective = \min\{TC; TR\} \quad (4)$$

Total Cost is obtained by the contribution of the costs associated with the three stages of the CCS system, namely Total Capture Cost *TCC* [€/y], Total Transportation Cost *TTC* [€/y], and Total Sequestration Cost *TSC* [€/y]:

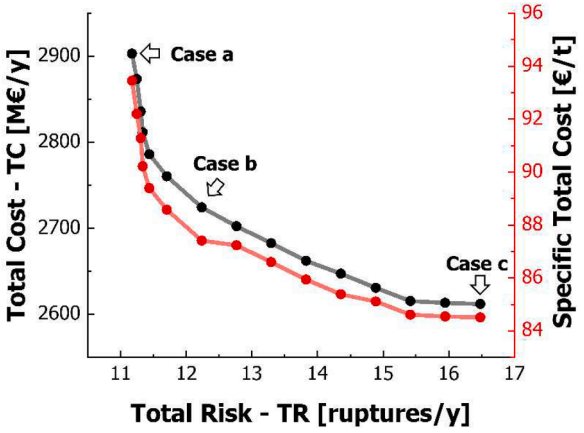

Fig. 9. Pareto front: Scenario I.3 (α = 80 % carbon reduction target): obtained through epsilon constraint method. Case a, Case b, Case c representing the three trade-off solutions (between the two objective functions: total cost TC [M€/y] and total seismic risk TR [ruptures/y]), to be discussed in detail.

$$TC = TCC + TTC + TSC \tag{5}$$

TCC is computed on the basis of the annual captured CO_2 flowrate $IN_{k,n}$ [t/y] through technology *k* in the emitting node *n*, representing the CO_2 inlet to the transport stage, and $CCA_{k,n}$ [€/t] the node-specific CO_2 avoidance cost through technology *k*:

$$TCC = \sum_{k,n} \left(IN_{k,n} \cdot CCA_{k,n} \right) \tag{6}$$

TTC is calculated based on the transported CO_2 flowrate $Q_{q,n,n'}$ through pipeline from node *n* to *n'*, the distance between nodes $LD_{n,n'}$ [km], UTC_p, the unitary cost factor tailored on set *p*, the offshore transport cost $UTC_{n,n'}^{offshore}$ defined as a matrix that takes the value of the multiplicative factor for offshore pipelines Ω [= 1.75] if the pipeline segment falls offshore, 1 otherwise, method described in the Supplementary Material, and the cost factor associated with the encountered obstacles $f_{n,n'}$:

$$TTC = \sum_{p,n,n'} \left(Q_{p,n,n'} \cdot LD_{n,n'} \cdot UTC_p \cdot UTC_{n,n'}^{offshore} \cdot f_{n,n'} \right) \tag{7}$$

TSC is given by the annual sequestered quantity of CO_2 OUT_n [t/y], i.e. the CO_2 outlet from pipelines, the unitary sequestration cost *USC*, and the additional costs for offshore storage $USC_n^{offshore}$ defined as a matrix that takes the value of Θ [= 2.5] if located offshore, 1 otherwise:

$$TSC = \sum_{n} \left(OUT_n \cdot USC \cdot USC_n^{offshore} \right) \tag{8}$$

TR is evaluated by summing up the $RR_{n,n'}$ [ruptures/y] concerning the pipelines in the transport network. $\lambda_{p,n,n'}$ is a binary variable that takes the value of 1 if a pipeline of size *p* is installed between nodes *n* and *n'*, 0 otherwise:

$$TR = \sum_{p,n,n'} \left(\lambda_{p,n,n'} \cdot RR_{n,n'} \right) \tag{9}$$

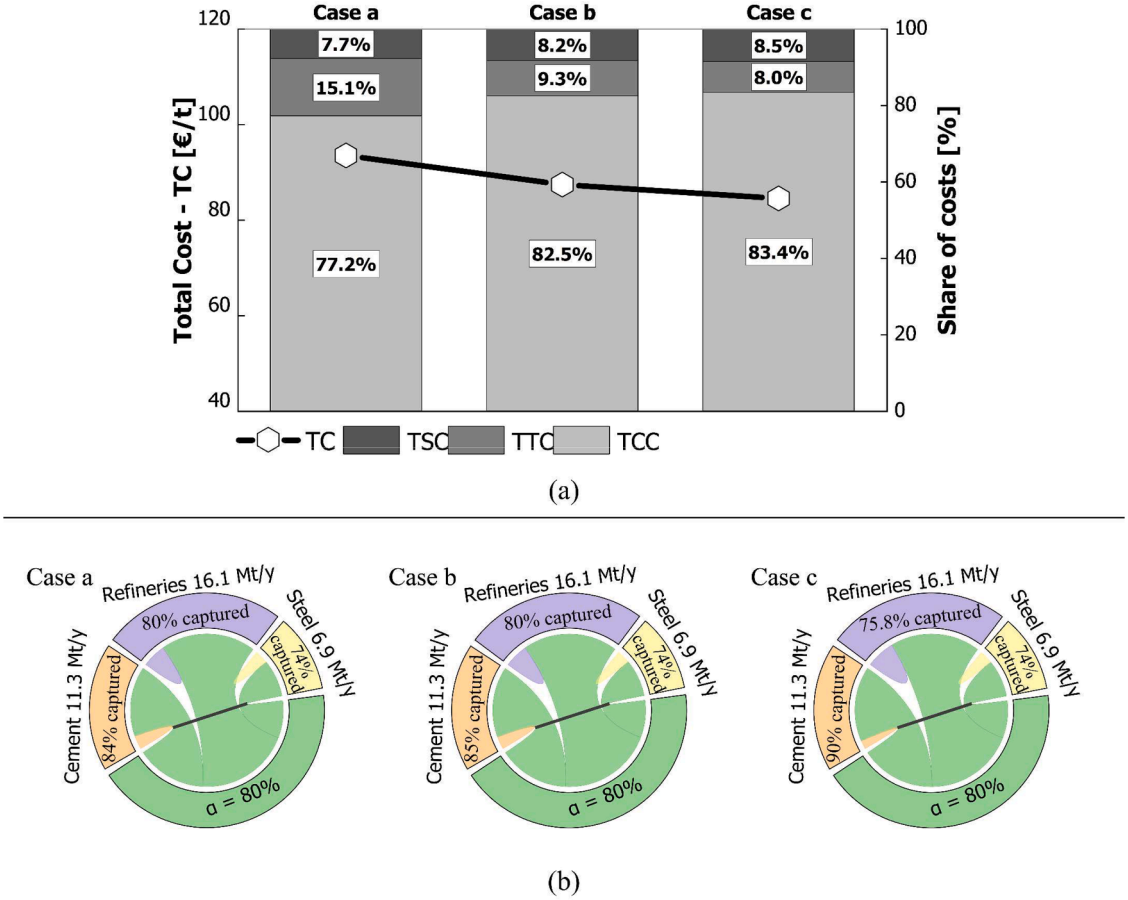

Fig. 10. Results for Scenario I.3: (a) Cost breakdown: TCC [%] capture cost, TTC [%] transport cost, TSC [%] sequestration cost (right y-axis), over total cost TC [€/t] (thick solid line, left y-axis); (b) Percentage of CO_2 captured from each sector, and the contribution of each sector to total CO_2 avoided through all technologies to reach the pre-set target of α = 80 % for the three Pareto optimal solutions (Case a, Case b, Case c).

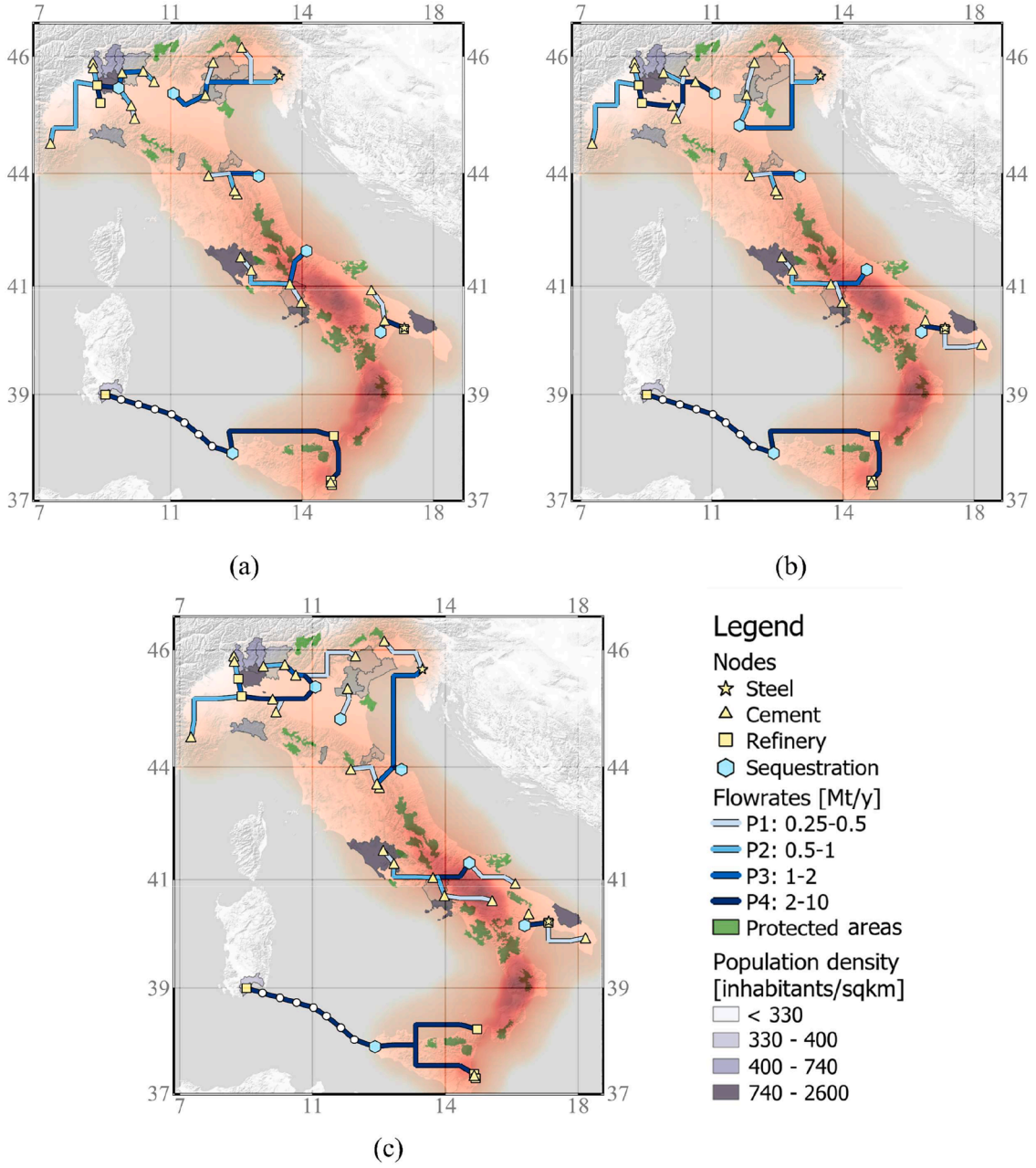

Fig. 11. Scenario I.3: CCS SCs configuration for (a) Case a: safest infrastructure, (b) Case b: trade-off configuration, (c) Case c: cheapest infrastructure.

All model equations are reported in the Supplementary Material.

3.3. Analysed scenarios

The multi-objective MILP model for CCS SC from the Italian industry was solved using the GAMS software (v. 38.3.0) with CPLEX solver. A pre-set carbon reduction target α is defined in the optimisation problem, considering the direct emissions from all sectors. Three Scenarios are defined and discussed.

Scenario I is formulated to determine the best CCS SC configuration in terms of both economic and seismic performance, allowing the model to sequester the captured CO_2 in both onshore or offshore geological formations in Italy. Based on different carbon reduction targets, three sub-scenarios are defined, namely Scenario I.1: $\alpha = 20$ %, Scenario I.2: $\alpha = 50$ %, and Scenario I.3 $\alpha = 80$ %. Scenario $\alpha = 80$ % represents a target close to the current technological limit for CO_2 capture.

Scenario II constrains the optimisation problem to offshore sequestration. Only the carbon reduction target $\alpha = 80$ % is considered. This investigation considers the fact that the public acceptance of CCS technologies improves when CO_2 is stored offshore (Mabon et al., 2015).

The methodology used to explore the Pareto front of optimal solutions between the conflicting objectives of economic optimum and seismic risk optimum is the ε-constraint method (Haimes, 1971). This Pareto front is determined for Scenario I only; for Scenario II, the results of the two objective functions are analysed separately. Total sequestered CO_2 is composed by the CO_2 flowrate that needs to be captured to reach the target α from all industrial sectors, plus the additional CO_2 emissions due to the capture plant (introduced into the modelling framework through parameter ρ_k). The different scenarios are summarised in Table 2.

4. Results

The optimisation was performed on a DELL Precision 7560 laptop

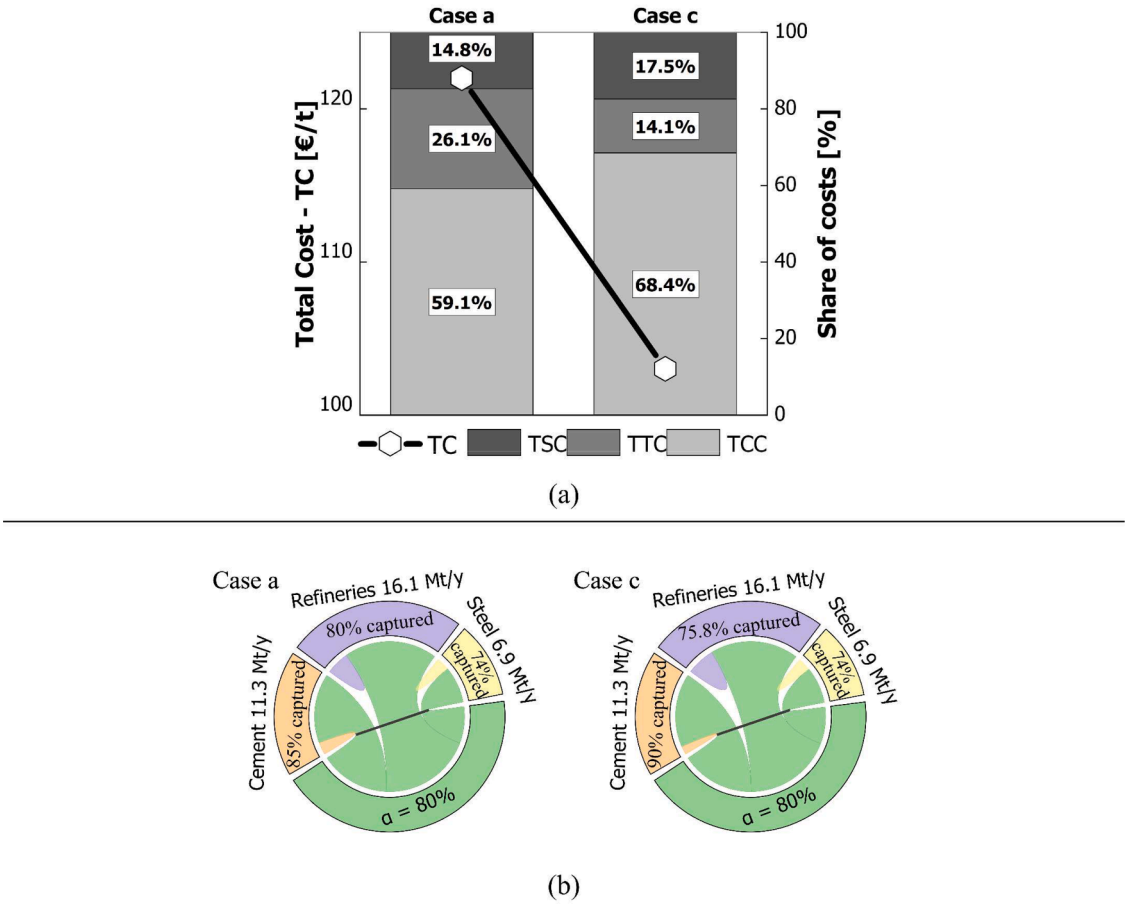

Fig. 12. Results for Scenario II: (a) Cost breakdown: TCC [%] capture cost, TTC [%] transport cost, TSC [%] sequestration cost (right y-axis), over total cost TC [€/t] (the latter represented by hexagons, left y-axis); (b) Percentage of CO_2 captured from each sector, and the contribution of each sector to total CO_2 avoided through all technologies to reach the pre-set target of α = 80 % for the two ideal Pareto optimal solutions (Case a, Case c).

with Intel(R) Core (TM) i7-11850H @ 2.50GHz 2.50 GHz and 64 GB RAM. Specifically, the MILP mathematical model was implemented in GAMS 38.3.0 and solved through CPLEX. The computation time varies from 20 s (in the case of 20 % target) up to 315 ks (in the case of 50 or 80 % target).

4.1. Scenario I: on shore and off shore sequestration

Scenario I aims at investigating the best configuration of a CCS SC in terms of both economic and seismic risk performance when varying the carbon reduction target from a value of $\alpha = 20$ % (Scenario I.1), $\alpha = 50$ % (Scenario I.2), until $\alpha = 80$ % (Scenario I.3). In all cases, the model has the option of choosing onshore or offshore sequestration in the Italian saline aquifers. For each Scenario (I.1, I.2, I.3), three Pareto optimal solutions were discussed, namely:

- *Case a*: the optimal solution in terms of seismic risk, representing the safest infrastructure;
- *Case b*: a trade-off solution between the two objective functions;
- *Case c*: the optimal solution in terms of economic performance, representing the least expensive infrastructure.

4.1.1. Scenario I.1: $\alpha = 20$ %

The economic and risk-related results are summarised in Table 3, and the Pareto front for Scenario I.1 ($\alpha = 20$ %) is presented in Fig. 3. *Case a* exhibits a total cost of 810 M€/y, corresponding to 98.3 €/t of CO_2, and is characterised by the safest infrastructure with a value of the total risk of 0.23 ruptures/y. The total pipeline length is 390 km. *Case c* represents the cheapest infrastructure, with a total cost of 410 M€/y (-49 % w.r.t. *Case a*), corresponding to 59.5 €/t of CO_2, and is characterised by the highest value of the total risk ($TR = 4.14$, i.e. 18 times higher than *Case a*). The total pipeline length is 786 km. *Case b*, among the set of all Pareto optimal solutions, is proposed as a reasonable trade-off between the two conflicting objectives, entailing a total cost of 475 M€/y, corresponding to 60.8 €/t of CO_2 and a total risk of 1.10 ruptures/y.

The cost breakdown of Scenario I.1, presented in Fig. 4(a), is intended to show the contribution of the three stages of a CCS infrastructure to the total cost, and, consistently with literature findings, it reveals that the capture stage contributes the most to the total cost, with a value of about 80 % in all the three cases. The transport stage contributes to about 10 % of the total cost in *Case a*, while in *Cases b* and *c*, it contributes to about 2 to 6 % due to the shorter total length of the pipeline system and, most importantly, because all transport pipelines are onshore. The sequestration stage weighs for about 7 % in *Case a* and around 12 % in *Cases b* and *c*.

The diagrams of Fig. 4(b) represent the percentages of captured CO_2 from the three different sectors (i.e. cement sector – representing 33 % of the total annual CO_2 emissions from Italian industry considered in the model, refinery sector – 47 % of the total annual CO_2 emissions, and steel sector – 20 % of the total yearly CO_2 emissions), and the contribution of each sector to the CO_2 avoided in order to meet the carbon reduction target of $\alpha = 20$ %. By analysing Fig. 4(b) and the CCS SC configuration presented in Fig. 5(a), some considerations can be drawn about *Case a*. It can be noticed that the captured CO_2 comes only from the refinery sector, 100 % of total CO_2 avoided. This makes sense in

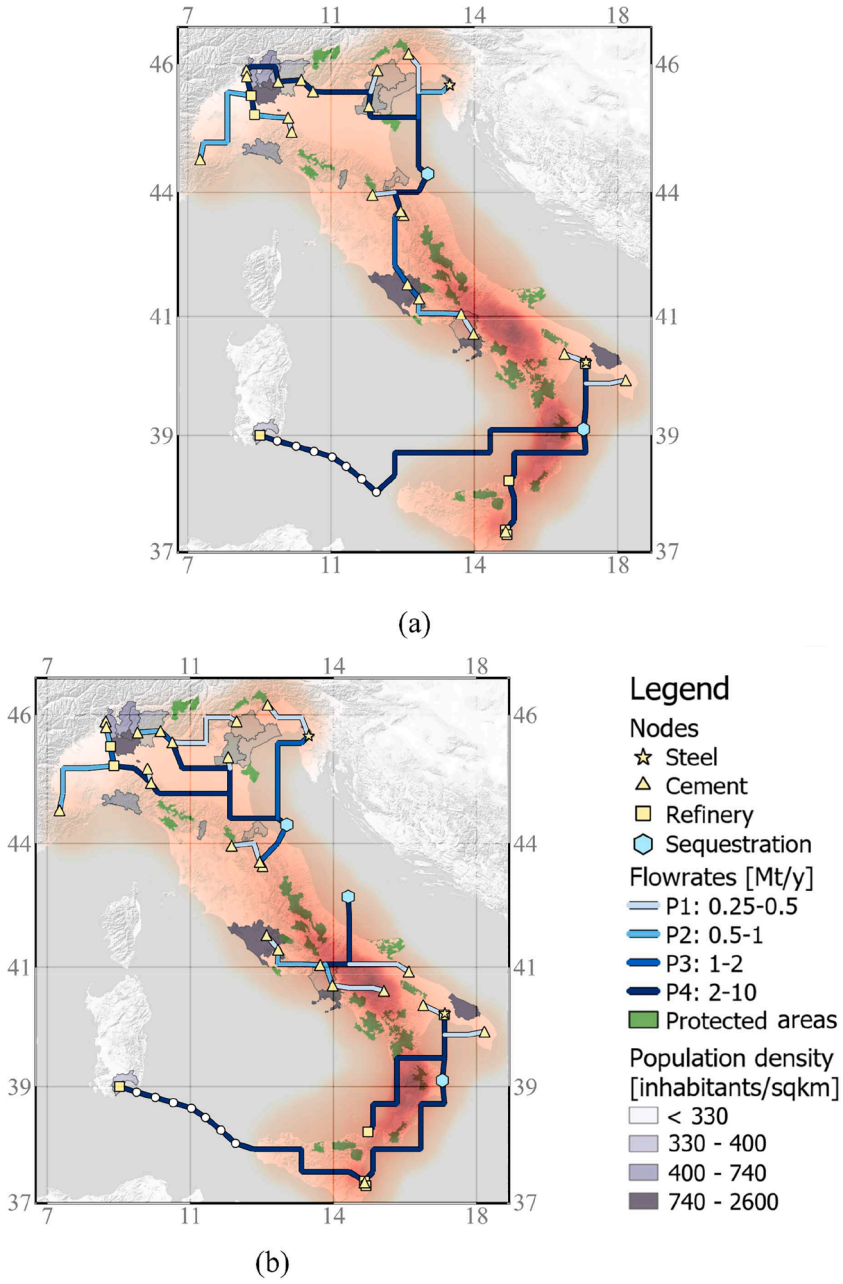

Fig. 13. Scenario II: CCS SCs configuration for (a) Case a: safest infrastructure, (b) Case c: cheapest infrastructure.

terms of seismic risk performance because *Case a* avoids smaller and distributed emission points (typically cement plants) in order to reduce onshore pipelines, and conversely favours large emission sites (typically refineries or steel plants) where capture is exploited to technological limits. Besides, the non-seismicity area in the south of Italy, i.e. the area between Sardinia and Sicilia, and the low-seismicity profile of Northern Italy are used as much as possible. For the Italian situation, this implies capturing CO_2 from refineries at full-scale (kr_3). The second major contribution to an increased total cost is due to the fact that the CO_2 captured at the refinery in Sardinia needs to be transported through offshore pipelines (transport cost is equal to 8.7 €/t).

Case c exhibits the best performance in terms of the total cost, but the worst performance in terms of seismic risk. By analysing Figs. 4(b) and 5 (c), it can be observed that the captured CO_2 comes mainly from cement plants and the steel sector, representing 71.6 % and 26.7 %, respectively, of total avoided CO_2, while the contribution of the refinery sector is only 1.8 %. In terms of economic performance, the pipeline network avoids protected areas and does not contain offshore transport. By doing so, the model chooses also options in areas with higher seismicity.

Case b shows a reasonable balance between total cost and total risk. This *Case* takes advantage of the low-seismic area of Southern Italy and installs a capture plant at the steel mill and refinery located there; however, a first-stage capture plant kr_1 (i.e. the cheaper capture option) is chosen for the refinery. This case avoids high seismic activity areas as well as protected areas.

4.1.2. Scenario I.2: $\alpha = 50$ %

In Fig. 6, *Case a* represents the safest CCS SC configuration (TR = 1.76 ruptures/y), with the highest cost (TC = 1682 M€/y with a specific total cost of 82.5 €/t), whereas *Case c* is the cheapest infrastructure (TC = 1250 M€/y with a specific total cost of 67.4 €/t), with the most vulnerable pipeline network in terms of seismic risk (TR = 16.35 ruptures/y). The total pipeline length is 788 km in *Case a* and 2921 km in *Case c*. *Case b*, i.e. the trade-off Pareto optimal solution, shows a

reasonable balance between the two objectives: a total cost of TC = 1404 M€/y (-16.5 % w.r.t. *Case a*) corresponding to a specific total cost of 73 €/t, and a total risk of TR = 5.61 ruptures/y (3 times lower w.r.t. *Case c*).

The cost breakdown of Scenario I.2 presented in Fig. 7(a) shows similar contributions as in Scenario I.1. The cost of the capture stage is about 80 % of the total cost in all three *Cases*, while the cost of transport varies from 8.5 % (*Case a*) to 12.2 % (*Case c*) of total cost; finally, the cost of sequestration contributes to about 8 % (*Case a*) up to almost 11 % (*Case c*).

By observing Figs. 7(b) and 8(a), it can be noticed that in *Case a,* CO_2 is captured from areas with low seismic activity (Northern Italy or Puglia) or no seismicity at all (Sardinia). Besides, CO_2 comes mainly from the refineries (4 out of 7 refineries included in the model, each with a full-scale capture plant: kr_3) with a share of 50 % of total CO_2 avoided, followed by CO_2 from the steel sector, representing 26 % of total CO_2 avoided through all other technologies (a full-scale capture plant is installed at the steel mill in Puglia). CO_2 captured from cement plants contributes to about 24 % of total CO_2 avoided (8 out of 23 cement plants are selected as capture nodes).

The shift in the main sources of CO_2 is clear when analysing *Case c*. Fig. 7(b) shows that the main source of CO_2 comes from the cement industry (all 23 cement plants are used to capture CO_2), representing 59 % of the total CO_2 avoided, while the shares of CO_2 coming from the refinery sector (all 7 refineries have a first step capture plant kr_1) drops to 10 % of total CO_2 avoided. The noticeably higher seismic risk of the transport network of *Case c* is mainly due to the fact that the cement plants are distributed all across the Italian peninsula, also in areas with high seismic activity.

As regards *Case b* of Scenario I.2, from Fig. 7(b) it can be observed that the percentage of CO_2 emissions captured through the different technologies is more balanced: 43 %, 31 % and 26 % of the total avoided CO_2 comes from cement plants, refinery sector and steel sector, respectively.

4.1.3. Scenario I.3: α = 80 %

Fig. 9 shows the Pareto Curve for Scenario I.3. *Case a*, the safest infrastructure (TR = 11.17 ruptures/y), gives the highest total cost (TC = 2903 M€/y, corresponding to a specific total cost of 93.5 €/t); the total pipeline length is 2347 km. *Case c*, the cheapest infrastructure (TC = 2612 M€/y, and a specific total cost of 84.5 €/t), gives the highest value for the total risk (TR = 16.48 ruptures/y); the total pipeline length is 2979 km. The trade-off configuration *Case b* entails a total cost TC = 2724 M€/y (the specific total cost is 87.4 €/t) and a total risk TR = 12.23 ruptures/y.

The cost breakdown is presented in Fig. 10(a), showing again that the main contribution is due to the cost of the capture stage. In this scenario, the capture cost does not vary significantly when comparing *Case a* with *Case c*: this makes sense since the capture infrastructure is run at (nearly) full capacity. However, the transport cost has a larger contribution in *case a* compared to the other cases. In fact, the difference between *cases a* and *b* mostly depends on the configuration of the transport infrastructure (apart from a small change in the selection of the cement plants). As presented in Fig. 10(b), the contribution of the steel sector to the total CO_2 avoided is constant throughout the three cases, using full-scale capture plants kr_3 for both steel mills considered in the model. The only difference that can be observed is related to the percentages of CO_2 avoided from cement plants and refineries. Similar to previous scenarios, *Case a* installs full-size capture plants in all 7 refineries, capturing all the possible CO_2 from this sector, while it chooses to capture CO_2 from 21 cement plants out of 23. In *Case c,* all possible CO_2 coming from the cement industry is captured, while in the case of refineries, around 75.8 % of the CO_2 emissions is captured, using both second step kr_2, and full-size capture plants kr_3. This also explains the much higher total pipeline length in *Case c*, since cement plants are more distributed.

The three CCS SC configurations are presented in Fig. 11(a,b,c). *Case a* finds the fastest transport route from a capture node to a sequestration node, avoiding long distances, and focuses on Northern Italy and Sardinia, as well as on the refinery and steel mill in Puglia. On the other hand, *Case c* captures all CO_2 from cement plants, regardless of location. Also, the transport network of *Case c* avoids all protected areas, such as national parks, high population density areas, and higher altitudes. *Case b* chooses to capture CO_2 from 20 out of 23 cement plants in areas with lower seismicity, and on the other hand, chooses transport arcs that are not located in high elevation areas or high population density areas to decrease transport costs.

4.2. Scenario II: considering only off shore sequestration – α = 80 %

Scenario II simulates the situation where only offshore sequestration in the Italian saline aquifers is allowed for a target of α = 80 %. At the Italian level, three offshore deep saline aquifers are identified. Only the seismic risk and economic optima (*Cases a* and *c*) will be discussed. *Case a*, the safest infrastructure with a total risk TR = 17.03 ruptures/y, entails a total cost TC = 3801 M€/y (corresponding to a specific total cost of 122 €/t); *Case c*, the cheapest infrastructure with a total cost TC = 3182 M€/y (-16.3 % w.r.t. *Case a* corresponding to a specific total cost of 103 €/t), exhibits the highest value of the total risk TR = 25.50 ruptures/y (1.5 times higher w.r.t. *Case a*).

The cost breakdown for Scenario II is presented in Fig. 12(a). Differently from Scenario I.3, now the contribution of transport and sequestration becomes more relevant. While the value of the total capture cost (*TCC*) in all three cases of Scenario II is comparable to the values presented in Scenario I.3, the values for total transport cost (*TTC*) and total sequestration cost (*TSC*) show a significant difference. In this situation, total capture cost (*TCC*) contributes to the total costs with 59 % in *Case a*, and 68 % in *Case c*. In terms of total transport cost (*TTC*), a significant difference is observed when analysing the two cases: *TTC* contributes to the total cost (*TC*) with 26.1 % in *Case a*, and 14.1 % in *Case c*. The higher contribution of transport cost in *Case a* can be explained by looking at the CCS SC configuration in Fig. 13(a): the pipeline network is preferably installed in low seismicity areas (Northern Italy), where the pipeline network crosses different obstacles that increase the total transport cost, i.e. high elevation areas, high population density areas and national parks, and in Sardinia, where it transports high CO_2 flowrates via offshore pipelines.

A significant increase is observed in the shares of total sequestration cost (*TSC*), which contribute to the total cost with 14.8 %, and 17.5 % in *Case a* and *Case c,* respectively. This is also an expected result due to increased sequestration costs in offshore sites.

Fig. 13(b), related to Scenario II, shows very similar results as the ones presented in Scenario I.3. The sectorial contribution to the total CO_2 avoided shifts from capturing all CO_2 from refineries in the more expensive *Case a*, to capturing all CO_2 from cement plants in *Case c*, while the percentage of CO_2 coming from the steel sector remaining unchanged, capturing all CO_2 from this sector.

5. Discussion

While our study on the optimal design of carbon capture and sequestration infrastructure in Italy offers valuable insights into the total cost and seismic risk considerations, it is important to acknowledge some simplifications and limitations.

First of all, pipeline trajectories are represented in a simplified way, assuming a straight-line pipeline installation between adjacent nodes, overlooking the complexities in pipeline routing. This is sufficient for a broad-scale analysis as the one carried out in this work; clearly it is not enough to design the network layout and to estimate detailed costs in the infrastructure deployment. Similarly, this study does not take into consideration site-specific data, which may be related to specific technologies and/or geographical constraints, and it assumes equal costs for plants in different locations. Also, this is a static study, which does not

consider the operational dynamics of processes, capture plants, and transport operations. Incorporating such dynamics would make the problem computationally intractable. However, notice that the inclusion of dynamic behaviours in the model would not significantly affect the main outcomes, which are associated to the optimal design of a full-scale infrastructure based on nominal levels of emissions, rather than on the operation of such systems under load variations.

A simplification is related to the exclusion of ships as transportation mode, too. We decided to consider only pipelines in this study for two reasons: (i) ship transport would not provide any additional insights into the seismic risk formulation as it is performed offshore; and (ii) given the geographic scale and the transported quantities of CO_2 in this study, ship transport would likely be more expensive than transport via pipelines as discussed in previous studies (IEAGHG, 2020).

This work focuses on seismic risk, representing one critical component of all credible risk scenarios affecting pipelines. The rupture of the pipeline can give rise to a loss of containment of carbon dioxide with subsequent impact on the population and the environment. This study does not investigate the evolution of the loss of containment since the adopted grid resolution does not allow for substantial assessment, requiring a more detailed insight into local conditions. Furthermore, other sources of societal risks (e.g. pipeline leakages) are not taken into account.

Another limitation is concerned with the definition of suitable sequestration sites. Geological storage sites in the Mediterranean area exhibit an early-stage degree of investigation, making other locations (e.g., the North Sea as in the Northern Lights project) more realistic candidates for CO_2 geological confinement. At the same time, transporting the CO_2 from Italy to the North Sea would require the setting up of a complex offshore infrastructure (probably based on ships), which would lead to a substantial increase in costs, compared to exploiting those basins located nearby the Peninsula, which can be reached via short offshore pipelines. In this sense, our work focusses on these less studied (and unexploited, yet) geological basins to provide a long-term perspective on how a CCS infrastructure in this area may look like while acknowledging the presence of seismic risk.

Finally, it is important to note that the study does not consider the political aspects nor delve into the policy implications of implementing a CCS infrastructure. The focus of the study is primarily on the economic and seismic risk aspects of designing such an infrastructure. While policy considerations play a significant role in the real-world implementation of CCS, they are beyond the scope of our study.

6. Conclusions

This study proposes a nation-wide, multi-objective, mixed integer linear programming optimisation framework for the optimal design of carbon capture and sequestration chains in terms of total cost and seismic risk, to assess the trade-off between these two conflicting objective functions and the effects on the design of such a large-scale infrastructure.

It emerges that by increasing the carbon reduction target (i.e., the ratio between the target CO_2 captured and the total one produced by the industrial plants considered in the model), the cost advantage of configurations based on economic optimisation over the safest ones decreases. For instance, for a 20 % reduction target, the safest design is 65 % more expensive than the one with the lowest cost (98.3 vs. 59.5 €/t), whereas, for an 80 % reduction target, this spread lowers to about 11 % (93.5 vs. 84.5 €/t). This depends on the fact that an ambitious CO_2 reduction target requires: i) to abate CO_2 emissions also in plants where capture costs are higher, and ii) to deploy an extensive and complex transport infrastructure. As a consequence, the safest design is comparable to its corresponding best economic network in terms of overall costs. On the other hand, cost-optimal solutions always determine a significant increase in seismic risk (between 1.5 and 18 times). It was also verified that the choice of limiting CO_2 sequestration to offshore basins determines an increase in the specific total cost, which is mainly driven by the transport and sequestration stages that account altogether to over 30 % (up to over 40 %) of total costs, compared to less than 20 % when also onshore capacities are included as a sequestration option.

CRediT authorship contribution statement

Daniel Crîstiu: Investigation, Methodology, Software, Visualization, Writing – original draft. **Federico d'Amore:** Conceptualization, Methodology, Writing – review & editing. **Paolo Mocellin:** Methodology, Writing – review & editing. **Fabrizio Bezzo:** Conceptualization, Methodology, Supervision, Writing – review & editing.

Declaration of Competing Interest

The authors declare that they have no known competing financial interests or personal relationships that could have appeared to influence the work reported in this paper.

Data availability

Data will be made available on request.

Supplementary materials

Supplementary material associated with this article can be found, in the online version, at doi:10.1016/j.ijggc.2023.103993.

References

ALA, 2001. Seismic fragility formulations for water systems. American Lifeline Alliance. ASCE, Washington, DC.

Allen, T.I., Wald, D.J., 2007. Topographic slope as a proxy for seismic site-conditions (VS30) and amplification around the globe. Open File Rep. https://doi.org/10.3133/ofr20071357.

Al-Yaeeshi, A.A., Al-Ansari, T., 2022. Developing operational resilience within CO2 utilisation networks: Towards ensuring business continuity through risk management. Comput. Chem. Eng. 161 https://doi.org/10.1016/j.compchemeng.2022.107746.

Argyroudis, S.A., Pitilakis, K.D., 2012. Seismic fragility curves of shallow tunnels in alluvial deposits. Soil Dyn. Earthq. Eng. 35, 1–12. https://doi.org/10.1016/j.soildyn.2011.11.004.

Becattini, V., Gabrielli, P., Antonini, C., Campos, J., Acquilino, A., Sansavini, G., Mazzotti, M., 2022. Carbon dioxide capture, transport and storage supply chains: optimal economic and environmental performance of infrastructure rollout. Int. J. Greenh. Gas Control 117. https://doi.org/10.1016/j.ijggc.2022.103635.

Bjerketvedt, V.S., Tomasgard, A., Roussanaly, S., 2022. Deploying a shipping infrastructure to enable carbon capture and storage from Norwegian industries. J. Clean. Prod. 333 https://doi.org/10.1016/j.jclepro.2021.129586.

Bui, M., Adjiman, C.S., Bardow, A., Anthony, E.J., Boston, A., Brown, S., Fennell, P.S., Fuss, S., Galindo, A., Hackett, L.A., Hallett, J.P., Herzog, H.J., Jackson, G., Kemper, J., Krevor, S., Maitland, G.C., Matuszewski, M., Metcalfe, I.S., Petit, C., Puxty, G., Reimer, J., Reiner, D.M., Rubin, E.S., Scott, S.A., Shah, N., Smit, B., Trusler, J.P.M., Webley, P., Wilcox, J., mac Dowell, N., 2018. Carbon capture and storage (CCS): the way forward. Energy Environ. Sci. 11, 1062–1176. https://doi.org/10.1039/C7EE02342A.

CEPCI, 2018. Chemical Engineering Plant Cost Index [WWW Document]. https://www.chemengonline.com/pci-home.

Chen, S., Liu, J., Zhang, Q., Teng, F., McLellan, B.C., 2022. A critical review on deployment planning and risk analysis of carbon capture, utilization, and storage (CCUS) toward carbon neutrality. Renew. Sustain. Energy Rev. 167, 112537 https://doi.org/10.1016/j.rser.2022.112537.

d'Amore, F., Bezzo, F., 2017. Economic optimisation of European supply chains for CO2 capture, transport and sequestration. Int. J. Greenh. Gas Control 65, 99–116. https://doi.org/10.1016/j.ijggc.2017.08.015.

d'Amore, F., Lovisotto, L., Bezzo, F., 2020. Introducing social acceptance into the design of CCS supply chains: a case study at a European level. J. Clean. Prod. 249 https://doi.org/10.1016/j.jclepro.2019.119337.

d'Amore, F., Mocellin, P., Vianello, C., Maschio, G., Bezzo, F., 2018. Economic optimisation of European supply chains for CO 2 capture, transport and sequestration, including societal risk analysis and risk mitigation measures. Appl. Energy 223, 401–415. https://doi.org/10.1016/j.apenergy.2018.04.043.

d'Amore, F., Romano, M.C., Bezzo, F., 2021a. Carbon capture and storage from energy and industrial emission sources: a Europe-wide supply chain optimisation. J. Clean. Prod. 290 https://doi.org/10.1016/j.jclepro.2020.125202.

d'Amore, F., Romano, M.C., Bezzo, F., 2021b. Optimal design of European supply chains for carbon capture and storage from industrial emission sources including pipe and ship transport. Int. J. Greenh. Gas Control 109. https://doi.org/10.1016/j.ijggc.2021.103372.

Donda, F., Volpi, V., Persoglia, S., Parushev, D., 2011. CO2 storage potential of deep saline aquifers: the case of Italy. Int. J. Greenh. Gas Control 5, 327–335. https://doi.org/10.1016/j.ijggc.2010.08.009.

EEA, 2020. European pollutant release and transfer register [WWW Document]. https://www.eea.europa.eu/data-and-maps/data/member-states-reporting-art-7-under-the-european-pollutant-release-and-transfer-register-e-prtr-regulation-23/european-pollutant-release-and-transfer-register-e-prtr-data-base.

Eidinger, J., n.d. Lifelines, water distribution systems in the Loma Prieta, California, earthquake of October 17, 1989. Performance of the built environment – Lifelines US Geological Survey Professional Paper 1552-A, 63-80.

EU GeoCapacity Project, 2009. Assessing European capacity for geological storage of carbon dioxide [WWW Document]. www.geology.cz/geocapacity/publications.

Gardarsdottir, S.O., de Lena, E., Romano, M., Roussanaly, S., Voldsund, M., Pérez-Calvo, J.F., Berstad, D., Fu, C., Anantharaman, R., Sutter, D., Gazzani, M., Mazzotti, M., Cinti, G., 2019. Comparison of technologies for CO2 capture from cement production—part 2: cost analysis. Energies 12. https://doi.org/10.3390/en12030542.

Gehl, P., Desramaut, N., Réveillère, A., Modaressi, H., 2014. Fragility functions of gas and oil networks. Geotech. Geol. Earthq. Eng. https://doi.org/10.1007/978-94-007-7872-6_7.

Germoso, C., Gonzalez, O., Chinesta, F., 2021. Seismic vulnerability assessment of buried pipelines: a 3D parametric study. Soil Dyn. Earthq. Eng. 143, 106627 https://doi.org/10.1016/j.soildyn.2021.106627.

Haimes, Y.Y., 1971. On a bicriterion formulation of the problems of integrated system identification and system optimization. IEEE Trans. Syst. Man Cybern. 1, 296–297.

Herzog, H., Javedan, H., 2009. Development of a Carbon Management Geographic Information System (GIS) for the United States. Pittsburgh, PA, and Morgantown, WV (United States). 10.2172/974322.

Ho, M.T., Bustamante, A., Wiley, D.E., 2013. Comparison of CO2 capture economics for iron and steel mills. Int. J. Greenh. Gas Control 19, 145–159. https://doi.org/10.1016/j.ijggc.2013.08.003.

Honegger, D.G., Wijewickreme, D., 2013. Seismic risk assessment for oil and gas pipelines, in: handbook of seismic risk analysis and management of civil infrastructure systems. Elsevier 682–715. https://doi.org/10.1533/9780857098986.4.682.

IEAGHG, 2017. understanding the cost of retrofitting co2 capture in an integrated oil refinery [WWW Document]. https://ieaghg.org/publications/technical-reports/reports-list/10-technical-reviews/819-2017-tr8-understanding-the-cost-of-retrofitting-co2-capture-in-an-integrated-oil-refinery.

IEAGHG, 2020. The status and challenges of CO2 shipping infrastructures. https://ieaghg.org/ccs-resources/blog/new-ieaghg-report-the-status-and-challenges-of-co2-shipping-infrastructures.

IPCC, 2022. Mitigation of Climate Change Climate Change 2022 Working Group III contribution to the Sixth Assessment Report of the Intergovernmental Panel on Climate Change. Cambridge University Press, Cambridge, UK and New York, NY, USA. https://doi.org/10.1017/9781009157926.

IPCC, 2005. IPCC Special Report on Carbon Dioxide Capture and Storage. Prepared by Working Group III of the Intergovernmental Panel on Climate Change. Cambridge University Press, Cambridge, United Kingdom and New York, NY, USA.

ISTAT, 2022a. Demografia in cifre [WWW Document]. https://demo.istat.it/.

ISTAT, 2022b. Confini delle unità amministrative a fini statistici [WWW Document]. https://www.istat.it/it/archivio/222527.

Italian Government, 2010. Elenco ufficiale delle aree naturali protette [WWW Document]. https://www.mite.gov.it/pagina/elenco-ufficiale-delle-aree-naturali-protette-0.

Kegl, T., Čuček, L., Kovač Kralj, A., Kravanja, Z., 2021. Conceptual MINLP approach to the development of a CO2 supply chain network – simultaneous consideration of capture and utilization process flowsheets. J. Clean. Prod. 314 https://doi.org/10.1016/j.jclepro.2021.128008.

Kim, C., Kim, K., Kim, J., Ahmed, U., Han, C., 2018. Practical deployment of pipelines for the CCS network in critical conditions using MINLP modelling and optimization: a case study of South Korea. Int. J. Greenh. Gas Control 73, 79–94. https://doi.org/10.1016/j.ijggc.2018.03.024.

Lanzano, G., Salzano, E., Santucci de Magistris, F., Fabbrocino, G., 2014. Seismic vulnerability of gas and liquid buried pipelines. J. Loss Prev. Process Ind. 28, 72–78. https://doi.org/10.1016/j.jlp.2013.03.010.

Lanzano, G., Santucci de Magistris, F., Fabbrocino, G., Salzano, E., 2015. Seismic damage to pipelines in the framework of Na-Tech risk assessment. J. Loss Prev. Process Ind. 33, 159–172. https://doi.org/10.1016/j.jlp.2014.12.006.

Lee, S.Y., Lee, J.U., Lee, I.B., Han, J., 2017. Design under uncertainty of carbon capture and storage infrastructure considering cost, environmental impact, and preference on risk. Appl. Energy 189, 725–738. https://doi.org/10.1016/j.apenergy.2016.12.066.

Mabon, L., Shackley, S., Blackford, J.C., Stahl, H., Miller, A., 2015. Local perceptions of the QICS experimental offshore CO2 release: results from social science research. Int. J. Greenh. Gas Control 38, 18–25. https://doi.org/10.1016/j.ijggc.2014.10.022.

Mina, D., Forcellini, D., Karampour, H., 2020. Analytical fragility curves for assessment of the seismic vulnerability of HP/HT unburied subsea pipelines. Soil Dyn. Earthq. Eng. 137, 106308 https://doi.org/10.1016/j.soildyn.2020.106308.

NETL, 2015. Cost and performance baseline for fossil energy plants Volume 1a: bituminous coal (PC) and natural gas to electricity. Revision 3 [WWW Document]. https://www.netl.doe.gov/projects/files/CostandPerformanceBaselineforFossilEnergyPlantsVolume1aBitCoalPCandNaturalGastoElectRev3_070615.pdf.

Nguyen, T.B.H., Leonzio, G., Zondervan, E., 2021. Supply chain optimization framework for CO2capture, utilization, and storage in Germany. Phys. Sci. Rev. https://doi.org/10.1515/psr-2020-0054.

O'Rourke, M., Ayala, G., 1993. Pipeline damage due to wave propagation. J. Geotech. Eng. 119, 1490–1498. https://doi.org/10.1061/(ASCE)0733-9410(1993)119:9(1490).

O'Rourke, M., Deyoe, E., 2004. Seismic damage to segmented buried pipe. Earthq. Spectra 20, 1167–1183. https://doi.org/10.1193/1.1808143.

Ostovari, H., Müller, L., Mayer, F., Bardow, A., 2022. A climate-optimal supply chain for CO2 capture, utilization, and storage by mineralization. J. Clean. Prod. 360 https://doi.org/10.1016/j.jclepro.2022.131750.

Rubin, E.S., Davison, J.E., Herzog, H.J., 2015. The cost of CO2 capture and storage. Int. J. Greenh. Gas Control 40, 378–400. https://doi.org/10.1016/j.ijggc.2015.05.018.

Stucchi, M., Meletti, C., Montaldo, V., Crowley, H., Calvi, G.M., Boschi, E., 2011. Seismic hazard assessment (2003-2009) for the Italian building code. Bull. Seismol. Soc. Am. 101, 1885–1911. https://doi.org/10.1785/0120100130.

Tromans, I., 2004. Behavior of Buried Water Supply Pipelines in Earthquake Zones (PhD Thesis). University of London.

Tsinidis, G., di Sarno, L., Sextos, A., Furtner, P., 2020. Optimal intensity measures for the structural assessment of buried steel natural gas pipelines due to seismically-induced axial compression at geotechnical discontinuities. Soil Dyn. Earthq. Eng. 131, 106030 https://doi.org/10.1016/j.soildyn.2019.106030.

van Straelen, J., Geuzebroek, F., Goodchild, N., Protopapas, G., Mahony, L., 2010. CO2 capture for refineries, a practical approach. Int. J. Greenh. Gas Control 4, 316–320. https://doi.org/10.1016/j.ijggc.2009.09.022.

Voldsund, M., Gardarsdottir, S.O., de Lena, E., Pérez-Calvo, J.F., Jamali, A., Berstad, D., Fu, C., Romano, M., Roussanaly, S., Anantharaman, R., Hoppe, H., Sutter, D., Mazzotti, M., Gazzani, M., Cinti, G., Jordal, K., 2019. Comparison of technologies for CO2 capture from cement production—part 1: technical evaluation. Energies 12. https://doi.org/10.3390/en12030559.

Wei, Y.M., Kang, J.N., Liu, L.C., Li, Q., Wang, P.T., Hou, J.J., Liang, Q.M., Liao, H., Huang, S.F., Yu, B., 2021. A proposed global layout of carbon capture and storage in line with a 2°C climate target. Nat. Clim. Change 11, 112–118. https://doi.org/10.1038/s41558-020-00960-0.

Wijaya, H., Rajeev, P., Gad, E., 2019. Effect of seismic and soil parameter uncertainties on seismic damage of buried segmented pipeline. Transp. Geotech. 21, 100274 https://doi.org/10.1016/j.trgeo.2019.100274.

ZEP, 2011. The cost of CO2 storage: post-demonstration CCS in the EU [WWW Document]. https://www.globalccsinstitute.com/archive/hub/publications/119816/costs-co2-storage-post-demonstration-ccs-eu.pdf.